Chapter 22
Impact of Local Urban Climate on Building Energy Performance: Case Studies in Mendoza, Argentina

Carolina Ganem Karlen, Julieta Balter, and Noelia Liliana Alchapar

22.1 Introduction

Globally, the significant increases in populations in urban areas over the recent decades due to rapid urbanization have induced the formation of the local climate change. One of the major factors in this change is the urban heat island (UHI) effect, which describes the excess warmth of the urban atmosphere in comparison to the rural areas (Levermore et al. 2017). Around 3.5 billion people live in urban areas all over the world and by 2050 more than two-thirds of the urban population will live in cities (DOE 2017). And around two-thirds of global primary energy demand is attributed to urban areas, inducing 71% of global direct energy-related GHG emissions (IEA 2014). According to the fifth assessment report on climate change from the Intergovernmental Panel on Climate Change (IPCC 2014), there is no doubt that anthropogenic greenhouse gas emissions (GHG) are responsible for the current climate change. Rapid urbanization increases demand for energy and consequently GHG emissions in cities.

The combination of the projected population and economic growth together with climate change results in placing greater stress on vital resources in the future if there is a continuation of the business-as-usual scenario. The energy sector in urban areas could thus play an important role in tackling climate change and in decreasing the carbon/energy footprint of urban areas. To support climate action plans and achieve more sustainable and resilient cities, understanding and managing urban energy use is essential (UN 2017). However, most of the time, the climatic challenges (e.g., comfort, energy demand, energy systems) are assessed individually while they are likely to be interrelated and require a holistic understanding of the ecosystem and human activities and the built environment (its form and materials) (Moonen et al. 2012). To achieve cities' energy and climate goals, it is necessary to

C. Ganem Karlen (✉) · J. Balter · N. L. Alchapar
INAHE, CCT-CONICET, Mendoza, Argentina
e-mail: cganem@mendoza-conicet.gov.ar

M. Palme, A. Salvati (eds.), *Urban Microclimate Modelling for Comfort and Energy Studies*, https://doi.org/10.1007/978-3-030-65421-4_22

reduce energy use in buildings through energy conservation and efficiency improvements. Computational tools can model performance of buildings at the urban scale to provide quantitative insights for stakeholders and inform their decision-making on urban energy planning, as well as building energy retrofits at scale, to achieve efficiency, sustainability, and resilience of urban buildings (Hong et al. 2020).

In recent years, multiple software tools have been developed for the assessment of urban climate, building energy demand, thermal comfort, and energy systems. Building energy simulation (BES) programs are capable of modelling building energy performance in detail in a dynamic model (building energy models (BEM)). Whole building energy simulation (BES) models play a significant role in the design and optimization of buildings. Simulation models may be used to compare the cost-effectiveness of energy conservation measures (ECMs) in the design stage as well as assess various performance optimization measures during the operational stage. Nevertheless, these tools often address only one or two of these urban planning aspects (Mauree et al. 2019). It is clear that building thermal performance and its energy consumption are affected by the energy exchange processes taking place between the outer skin or envelope of the building and the surrounding environment. It is a dynamic system in which there are continuous changes in a daily and seasonal range. Quantity and quality of the exposed envelope as well as albedo, vegetation, and urban geometry are significant factors in determining the impact of urban microclimates on energy building consumption.

Many previous studies have documented significant impacts of the urban microclimate on the thermal loads, and thus building energy performance. For instance, the effects of UHI, a term raised by Manley (1958), might lead to changes to building energy demand (e.g., a decrease in heating but an increase in cooling) depending on the city, type of building, or meteorological conditions, which yield a wide range of impacts on energy consumption (Davies et al. 2008; Xu et al. 2012; van Hooff et al. 2016). An example is that the weather data collected at airports are commonly used for building energy simulations and these data do not take into account real temperature distribution in cities. A recent modelling study based on a building located in the center of Rome, Italy, indicated that the energy consumption of cooling would be underestimated by 35–50% if the climatic effect of the heat island is not considered (Ciancio et al. 2018; Zinzi et al. 2018). This report is consistent with the results found by Correa (2006) for the city of Mendoza, Argentina, located in a similar climate.

The existing methods and tools have limitations in representing a realistic urban energy model and supporting energy performance evaluation at urban or neighborhood scales. There is a lack of an integrated approach for modelling and analyzing different components of urban energy use. In simulation-based methods, oversimplification of the urban context, urban microclimate, and inter-building effects are the major limitations (Abbasabadi and Ashayeri 2019). The urban context is often simplified or neglected in building energy models (BEMs) due to the difficulties of taking accurately into account all the heat fluxes emanating from the environment. Oversimplifying the urban context can impact the accuracy of BEM predictions. Nevertheless, several approaches can be used to allow for the impact of the urban environment on the dynamic behavior of a building, its heating and cooling demands, and thermal comfort (Lauzet et al. 2019). Co-simulation between models is necessary to understand the impact of systems interacting with each other in real time (Hong et al. 2020).

With the aim of finding a solution, in the scientific field there are some experiences regarding the integration of two different scales in dynamic simulation programs: for the building scale by using EnergyPlus or TRNSYS (Transient Systems Simulation) and for the neighborhood scale by using ENVI-met. Yang et al. (2012) developed a simulation methodology to integrate ENVI-met and EnergyPlus programs, based on the mapping of the surfaces of a building. The work uses the Building Controls Virtual Test Bed (BCTVB) software to develop a coupling module in order to transfer the simulation results between the two programs. Morakinyo et al. (2016) worked on validating the urban model in ENVI-met with in situ measurements and then specific external meteorological data was used to create the object of "a design day" and apply it as a boundary condition for each building in the simulation with EnergyPlus. Pastore et al. (2017) performed a simulation with ENVI-met of a neighborhood in order to obtain climatic boundary conditions (without on-site measurements). The climatic variables were used to simulate the neighborhood on a smaller scale with different scenarios. Finally, the microclimatic output variables were used to simulate with EnergyPlus temperatures and indoor comfort conditions.

Moreover, Kuo-Tsang and Yi-Jhen (2017) used the two simulators mentioned above based on data from meteorological bases of a typical year to simulate the microclimatic conditions of urban canyons for the warmest climatic conditions of the year. Lassandro and di Turi (2019) evaluated the possibility of integration of EnergyPlus and ENVI-met by comparing external surface temperature values in three different cities obtained by in situ thermograph measurements. On a local scale, Balter et al. (2018) evaluated the predictive potential of ENVI-met as a tool for building thermal analysis in an arid climate context. The high degree of adjustment—R^2 above 0.94—of the indoor air temperature monitored and adjusted with EnergyPlus versus that used with the microclimatic data calculated with the urban simulator ENVI-met supports the reliability of the predictive results of the integration method of both software.

There are also examples of integration of ENVI-met and TRNSYS software. Schwed and Sheng (2017) applied an algorithm to translate climatic data (EPW) into annual databases for specific locations and microclimates through simulation with ENVI-met. This information was used to simulate thermal conditions and cooling demands in buildings through the TRNSYS program. Perini et al. (2017) incorporated CFD-based simulation tool ENVI-met and TRNSYS (Transient Systems Simulation) by means of Grasshopper. The results confirmed the potentialities of combining both software for the calculation of urban features affecting urban microclimate (urban form, vegetation, canyon proportion) incrementing the simulation accuracy in terms of outdoor thermal comfort, especially during night.

Due to the complexity of the built environment and prevalence of large numbers of independent interacting variables, it is difficult to achieve an accurate representation of real-world building operation. Even though existing buildings and their microclimates can be monitored in situ, this practice is very useful but time and resource consuming. Only some punctual cases can be evaluated thoroughly, and it is impossible to measure buildings that are still in project. Therefore, by reconciling model outputs with measured data, we can achieve more accurate and reliable results in simulations (Ganem Karlen 2006; Coakley et al. 2014). Regarding all of the expressed above, it is clear that to provide reliable estimates microclimate models need to be parameterized based on empirically obtained data.

This chapter deals with the comparison of microclimatic information obtained with different methods:

1. Local weather stations average climate data from the past 20 years. As averaged, they prevent visualization of increasing temperatures over time due to climate change.
2. On-site microclimatic measurements: Very expensive and time consuming but very accurate.
3. Results of ENVI-met software: They allow a reduction in time and costs with respect to in situ measurements. Prior validation is necessary.

A case study in a high-density area in the city of Mendoza, Argentina, is presented in which year-round in situ measurements of temperature, humidity, radiation, and air movement were taken in two different scales: within the streets in a neighborhood and outside and inside a building. The micro-urban scale and the building scale were covered. A specific weather file was created for each scale, to be integrated in simulation software ENVI-met and EnergyPlus, respectively. Models were calibrated with the real data, to be run again with the information provided by local weather stations. Also, as a third term of comparison, the simulation workflow moves from the micro-urban- to a building-scale assessment by linking the ENVI-met software microclimatic results to the building energy simulation program EnergyPlus.

Results obtained with the three alternatives—(a) with the local weather stations' average climate input, (b) with the on-site microclimatic measurements, and (c) with ENVI-met software—are compared in order to assess each case reliability in assessing the impact of local urban climate on building energy performance.

22.1.1 Application Case: Mendoza, Argentina

The city of Mendoza is located at the foot of the Andes Mountains, in central western Argentina (32° 40′ South Latitude, 68° 51′ West Longitude, and 750 m above sea level). Although Mendoza is located in a semiarid continental climate with low percentages of atmospheric relative humidity, high heliophany, and annual precipitation of 218 mm—BWk according to Köppen classification (Kottek et al. 2006)—it does not follow a compact urban model. Its urban model is defined by its wide and tree-lined streets that form green tunnels. The checkered frame contains the buildings while the main strategy for minimizing the sun exposure is the vegetal frame. Mendoza's urban structure intermingles three types of meshes that overlap in space: a water network, the characteristic Spanish regular orthogonal grid, and, finally, a green mesh that arises due to the interaction of the first two. See climatic data for the city of Mendoza, Argentina, in Table 22.1.

The analysis was carried out within a grid of 6 × 6 ha, which totals 36 blocks in Mendoza Metropolitan Area (MMA). This area, mainly for residential use, was selected because of its high building density with more than 800 inhabitants/ha. It includes the five main squares of the city: Independence, Chile, San Martin, Spain, and Italy. The building height ranges from 3 to 57 m, with a higher percentage of buildings between 1 and 3 levels.

The distribution of surfaces in the evaluated sector corresponds to 44% of roofs, 28% of vehicular roads, 10% of squares, and 18% of private uncovered surfaces (courtyards, gardens). With respect to the material configuration, there is a generalized use of the calcareous pedestrian pavement in different colors: yellow (31%), red (21%), black (11%), and gray cement (22%), among others, with an average albedo of 0.3. The opaque surface materials that make up the facades of the urban canyon are predominantly of stone, brick, and/or paintings. The average albedo of vertical materials is 0.2. Most of the roofs are flat (80%) mainly built in reinforced

Table 22.1 Climatic data for the city of Mendoza, Argentina

Annual values	Average maximum temperature	22.6 °C
	Average minimum temperature	11.0 °C
	Mean temperature	15.9 °C
	Global horizontal irradiance	18 MJ/m^2
	Relative humidity	54.7%
	Mean rainfall	218 mm
July (winter)	Average maximum temperature	14.7 °C
	Average minimum temperature	3.4 °C
	Mean temperature	7.8 °C
	Thermal amplitude	11.3 °C
	Global horizontal irradiance	9.9 MJ/m^2
	Mean wind velocity	7.6 km/h
January (summer)	Average maximum temperature	30.1 °C
	Average minimum temperature	18.4 °C
	Mean temperature	25.3 °C
	Thermal amplitude	11.7 °C
	Global horizontal irradiance	25.7 MJ/m^2
	Mean wind velocity	10.8 km/h
Annual heating degree-days (T_b = 18 °C)		1384
Annual cooling degree-days (T_b = 23 °C)		163

Source: SMN (2019)

concrete and silver waterproof membranes (average albedo = 0.3). The remaining 20% is tilt and constructed with red ceramic tiles (average albedo = 0.35) (Alchapar et al. 2014).

The trees planted in alignment in the city of Mendoza correspond 78% to three species: "white mulberry" (*Morus alba*) 38%; "London plane" (*Platanus hispanica*) 21%; and "European ash" (*Fraxinus excelsior)* 19%. The remaining 22% corresponds to "American ash" (*Fraxinus americana*), "*Senegalia visco*" (*Acacia visco*), "white cedar" (*Melia azedarach*), "tipa" (*Tipuana tipu*), "poplar" (*Populus* spp.), and "Acer" (*Acer negundo*) (Martinez et al. 2017).

22.2 Microclimate and Buildings

22.2.1 Design and Validation of the Numerical Model at Urban Scale with ENVI-met

The free access program ENVI-met 3.1, developed by Michael Bruse at the Geography Institute of the University of Mainz, Germany, was used to perform the numerical design. This three-dimensional computational model works on an urban microclimate scale and simulates the interactions between the air and the surface of the urban environment with a typical resolution of 0.5–10 m in space and every 10 s in time. ENVI-met 3.1 is based on the fundamental laws of fluid dynamics and thermodynamics. The model includes the simulation of flows around and between buildings; heat and steam exchange processes of floor and wall surfaces; turbulence; vegetation parameters; bioclimatology; and dispersion of pollutants (Bruse 2006).

The data input for the numerical modelling of the urban area evaluated can be divided into three groups:

– Design of the physical space: The model was made in a 200 × 200 × 30 version. The resolution of the area is 3.5 × 3.5 × 3 m and a mesh of 197 (x) and 197 (y) because the reference surface is 690 × 690 m.
– Climate variables: The ENVI-met 3.1 software requires the entry of undisturbed variables that characterize the simulation boundary conditions, such as (1) wind speed, wind direction (m/s) at 10 m height, and roughness from ground ($z0$) to the reference point; (2) initial atmospheric temperature (K) and specific humidity (gr. water/kg air) at 2500 m high: the data were obtained from Francisco Gabrielli Airport—Station n° 87418, Aero de Mendoza Observatory—in collaboration with the University of Wyoming; and (3) relative humidity (%) at 2 m height, registered with ONSET Weather sensor, type HOBO H08-003-02 (fixed point observed -Po-, for adjustment).

Table 22.2 Input parameters for simulation in ENVI-met

Data		December 19th
Main	Wind velocity at 10 m [m/s]	2
	Wind direction (0:N; 90:E; 180:S; 270:O)	150
	Roughness *z*0 to the reference point	0.1
	Initial atmospheric temperature [K]	295
	Specific humidity at 2500 m [gr. water/kg air]	2.8
	Relative humidity at 2 m [%]	35
Buildings	Interior temperature [K]	295
	Wall thermal transmittance [W/m^2 K]	2
	Roof thermal transmittance [W/m^2 K]	0.7
	Wall albedo	0.2
	Roof albedo	0.3
Ground	Initial temperature—top layer (0–20 cm) [K]	293
	Initial temperature—middle layer (20–50 cm) [K]	293
	Initial temperature—deep layer (below 50 cm) [K]	293
	Relative humidity—top layer (0–20 cm) [%]	50
	Relative humidity—middle layer (20–50 cm) [%]	60
	Relative humidity —deep layer (below 50 cm)	60
Number of meshes		*x*-Meshes: 197
		y-Meshes: 197
		z-Meshes: 23
Size of the mesh (m)		d*x*: 3.5
		d*y*: 3.5
		d*z*: 5
Vegetation		Tree 15 m light: Height 15 m
		LAD1: 0.04; LAD6: 0.150; LAD10: 0.00 (m^2/m^3)
		Tree 15 m very dense: Height 15.0 m
		LAD1: 0.15; LAD6: 2.15; LAD10: 0.00 (m^2/m^3)
Road pavement		Concrete: albedo 0.3
Sky view factor at point A	Building	0.648
	Building + vegetation	0.332

Source: Own elaboration (2019)

– Thermal properties of the urban theoretical model: For the characterization of buildings it is necessary to define internal temperature, thermal transmittance, albedo, conductivity, and specific heat of walls, roofs, and pavements. In order to specify the behavior of the soil, temperature and humidity must be specified for different soil layers. Table 22.2 lists the simulation conditions and the properties used.

22.2.1.1 Monitoring and Calibration

The microclimatic conditions of the area were monitored during the summer period of 2012–2013 by means of the fixed reference point (Po) located within the analyzed road channel and indicated in Fig. 22.1. The urban monitoring point (Po) was selected from a grid of available monitoring points in the city, because it is at a close distance (less than 500 m) from the reference building (Bo). Moreover, the orientation of the road channels where both sensors (Po and Bo) are located is coincident. Both channels have an E-O arrangement. Ruiz et al. (2017) have demonstrated that E-O is the most appropriate orientation for urban channels in the city of Mendoza, allowing full North exposure in building facades (towards the Equator in the South Hemisphere). Furthermore, road channels with E-O orientation represent almost between 55% and 60% of the city's frame.

To calibrate the numerical model, the air temperature curve was contrasted Po, with the air temperature curve of the simulated area with ENVI-met (Ps). December 19th was selected as reference day, as ENVI-met version 3.1 software allows calculating the microclimatic characteristics of a single reference day. See Fig. 22.2.

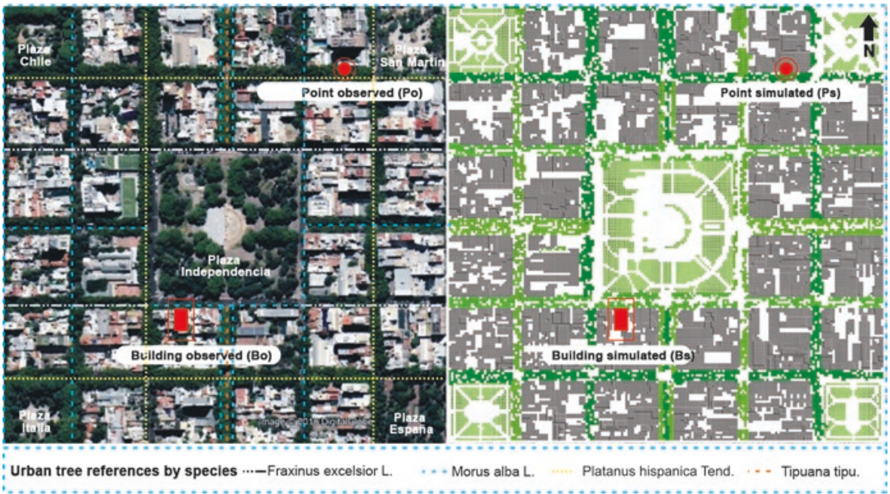

Fig. 22.1 Aerial view of the studied area and numerical model configuration with ENVI-met 3.1. Location of point observed (Po) and simulated (Ps), and building observed (Bo) and simulated (Bs). Description of urban trees. (Source: Own elaboration 2019)

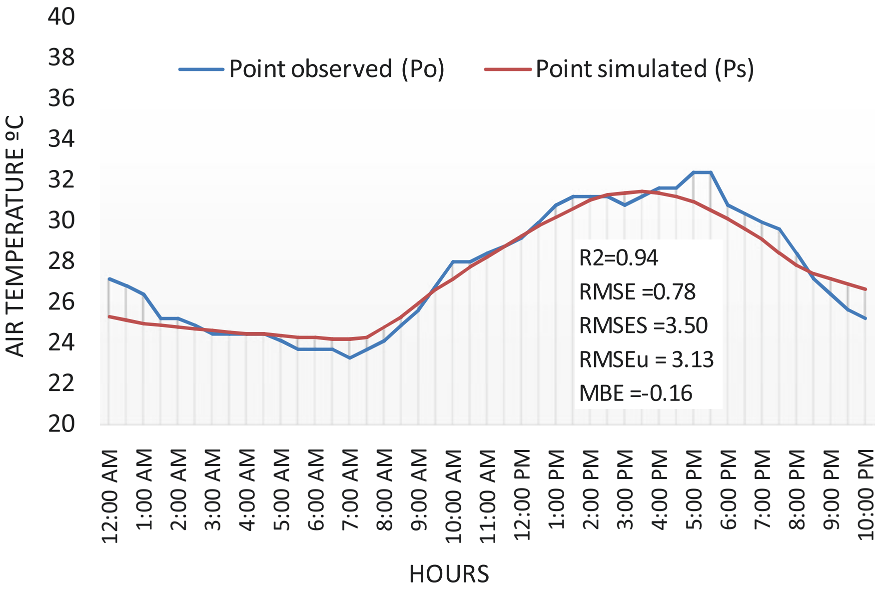

Fig. 22.2 Simulated (Ps) and observed (Po) point adjustment chart at a pedestrian scale (2.5 m) in the area for December 19th. (Source: Own elaboration 2019)

22.2.2 Design and Validation of the Numerical Model at Building Scale with EnergyPlus

The selected case is a north-facing building corresponding to the Tower typology. This typology corresponds to one of the three morphological classifications existing in Mendoza according to the building regulations at the time of its construction (Balter et al. 2013).

The monitored housing unit, located on the fifth level, has an area of 122 m^2 and location is frontal, that is, oriented to the public road and therefore to the urban forestry. Likewise, for its selection it was considered pertinent, since the building is implanted in front of a square that ensures the absence of shadows by the surroundings.

As for materiality, it is a mostly massive building, with 73% opaque materials in its envelope and 10% in the exposed reinforced concrete envelope (structure). The exterior walls are of 0.30 m hollow ceramic brick with plaster and paint without insulation and the interior divisions are of the same material of 0.10 m thickness. The glasses are simple 4 mm (K = 5.8 W/m^2 °C, solar factor = 0.87). As sun protection elements, the building has 1.20 m deep balconies and sliding shutters with white wooden lattices. See Fig. 22.3.

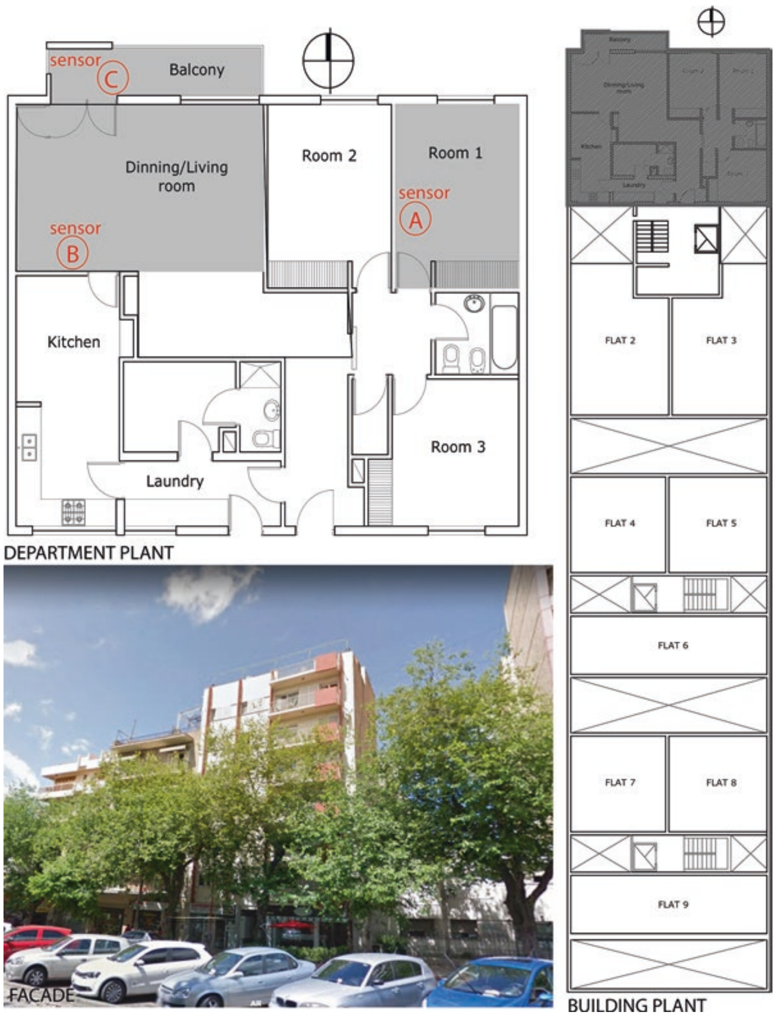

Fig. 22.3 Image and plan of the selected building. Plan of the monitored housing unit in three different heights: first floor, fifth floor, and eighth floor (upper level). (Source: Own elaboration 2019)

22.2.2.1 Monitoring and Calibration

On-site audits were carried out in a period from December 14th to January 10th. Micro-acquirers of HOBO U12 data of temperature and relative humidity were used and recording intervals were set every 15 min synchronously in all instruments, criteria adopted according to the recommendations of Longobardi and Hancock (2000). The sensors were installed in different environments: two inside (living room and bedroom) and one outside (balcony) protected from solar radiation. They were located at an average height of 2 m, following the recommendations of Kolher and Hassler (2002), and at a sufficient distance from the mass of the walls in order to avoid distortions in the data (Oke 2004).

The measurements made were used to validate the dynamic simulation model using the EnergyPlus program, version 8.8. This free program was developed by the Lawrence Berkeley National Laboratory (LBNL) and is currently the official simulation software of the US Department of Energy. Table 22.3 shows the description of the opaque materiality.

The validation was carried out in the fifth-level housing unit due, on the one hand, to the need to isolate the heating or cooling contributions inside the spaces: this unit was unoccupied, with windows and curtains closed, during the period of measurement; therefore, mechanical air-conditioning means were not used. This situation was observed in the audited thermal behavior and was corroborated in the interviews conducted with the users. The simulation was scheduled 10 days before the selected date as it is important that the physical model enters into regime in advance.

The climate file (EPW) used for the validation of the model was made with the temperature and relative humidity data monitored outside the building, and with the radiation data measured at the Mendoza Scientific and Technological Centre, which is located within a radius of 2.6 km, distance that is appropriate for the validity of

Table 22.3 Properties of the materials input for the EnergyPlus model

Layers	Roughness	Thickness (m)	Conductivity (W/m °C)	Density (kg/m^3)	Specific heat (J/kg °C)
Exposed envelope (structure)					
Concrete	Rough	0.12	1.7	2400	800
Exposed envelope (exterior walls)					
Exterior revetment	Very rough	0.025	0.93	1900	1000
Hollow ceramic brick	Rough	0.3	0.41	1200	600
Interior revetment	Very rough	0.025	0.93	1900	1000
Interior walls					
Exterior revetment	Very rough	0.025	0.93	1900	1000
Hollow ceramic brick	Rough	0.1	0.41	1200	600
Interior revetment	Very rough	0.025	0.93	1900	1000
Floors/ceilings					
Plaster	Smooth	0.025	0.48	741.3	836.3
Concrete	Rough	0.12	1.7	2400	800
Concrete mortar	Medium roughness	0.1	1.63	2400	800
Wooden floor	Smooth	0.025	0.11	500	2800

the data according to what is indicated for the solar radiation records of the Solarimetric Network of the Argentine Republic (Grossi Gallegos et al. 1983). Figure 22.4 shows the curves of the adjustment made in the living room, for the period from December 19th to December 21st.

22.2.3 Simulation of Energy Consumption and Temperatures for Houses Above and Below the Tree Canopy, According to Different External Microclimatic Data

The energy consumption simulations were carried out by programming 24 °C thermostats for all areas of the building in three identical housing units located in different relative positions in height within the monitored building. A height limit to define whether the housing unit is located above or below the tree canopy was defined based on the types of trees: 12 m from street level for "white mulberry" (*Morus alba*) which is considered as from the fourth story (12 m) of the building. The following indices were determined (Balter 2015):

– Housing below the tree canopy: up to and including the fourth story (ground floor +3), corresponds to a height up to 12 m
– Housing above the tree canopy: starting from the fifth story (ground floor +4), corresponds to a height greater than 12 m

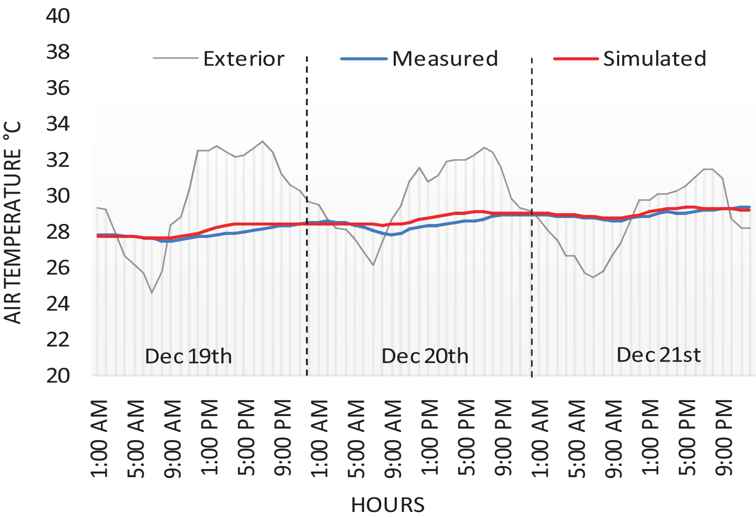

Fig. 22.4 Adjustment of the measurements in the EnergyPlus model for housing located above the tree canopy. (Source: Own elaboration 2019)

Three cases were defined to predict buildings' heating and cooling needs and energy consumption through the dynamic simulation method:

- *First floor* (under the tree canopy)
- *Fifth floor* (above the tree canopy) with adiabatic ground and roof because the housing unit is surrounded by other units under and above
- *Eighth and upper floor* (above the tree canopy) where the exposed envelope is extender because of the exposure of the roof to the microclimatic conditions

Predicting buildings' heating and cooling needs through dynamic simulation methods requires the input of hourly weather data, so as to represent the typical meteorological characteristics of a specific location. Hence, the so-called typical weather years (TWY), mainly deduced from multi-year records of meteorological stations outside the urban centers, cannot account for the complex interactions between solar radiation, wind speed, and high urban densities which lead to the formation of the urban heat island effect and to higher ambient air temperatures.

To take these facts into account, five different types of files (EPW extension) were formed for the entry of climatic data with the required data: global radiation on horizontal surface, diffuse radiation on horizontal surface, direct normal radiation to the beam, external dry bulb temperature, and external relative humidity, atmospheric pressure, and wind speed and direction. The data required for the conformation of the climate file (EPW) were repeated for the period of 10 days prior to the selected analysis date so that the model enters into regime with the calculated climatic variables. We worked with a total of five climate data files, according to the following configurations (see Fig. 22.5 for a location of the different points on the map):

1. Statistical data (Sd point): average climatic databases for a period of 14 years (2003–2017) from Francisco Gabrielli Airport—Station n° 87418, Mendoza Observatory, outside the city 8.6 km apart (OB Org 2019). In this case we worked with a single climate file, without differentiating the situation above and below the tree canopy.
2. Monitored building data (Bo point):

   2A. Temperature and relative humidity data obtained from measurements taken outside the monitored apartments above the tree canopy. Solar radiation data were those measured at the Mendoza Scientific and Technological Centre (CCT), 2.6 km apart.

   2B. Temperature and relative humidity data obtained from measurements taken outside the monitored apartments below the tree canopy. In order to contemplate the situation under the tree canopy, the incident radiation under the urban grove was affected with a local permeability factor. According to Cantón et al. (2003) global radiation permeability corresponding to the existing urban forestry in this case study (*Morus alba*) is 31.4% at midday in summer.

Sd point	To Airport whether station	8.6 Km
CCT point	To Scientific and to Technological Centre whether station	2.6 Km
Po Point	To Observed fixed point	0.7 Km

Fig. 22.5 Distance from building observed (Bo point). (Source: Own elaboration 2019)

3. Data calculated by ENVI-met (Po point): Two climate files were formed, based on the data obtained from the ENVI-met model for monitor points located in the road channel where the building is located, 0.7 km apart, simulated for December 19:

   3A. Above the tree canopy: for a height of 12.5 m
   3B. Below the tree canopy: for a height of 2.5 m

Figure 22.6 compares global radiation curves for each climatic model. Model 1 (statistical data) presents an averaged curve with a maximum value at midday of 1050 W/m^2. Model 2 (monitored building data) is with a maximum value at midday of 1067 W/m^2 (2A), which is reduced to 704 W/m^2 by the effect of the urban forestry in this case study (2B). Model 3 (data calculated by ENVI-met) is with values at midday of 1047 and 715 W/m^2 above and under the tree canopy, respectively (3A and 3B).

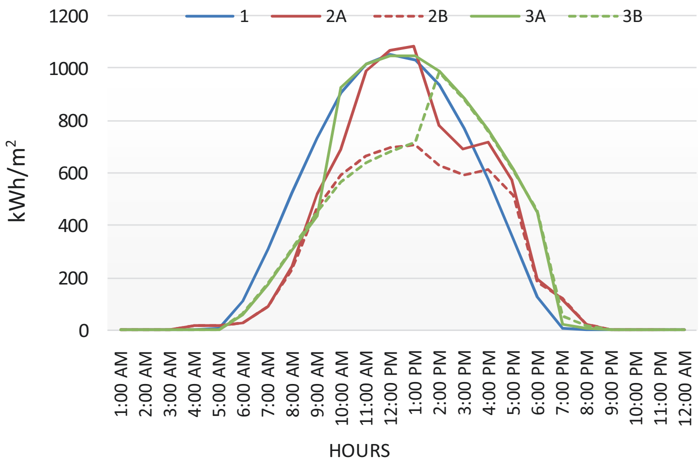

REFERENCES	1.Statistical data	2.Monitored data	3. Data calculated by ENVI-met
Above tree canopy	1	2A	3A
Below tree canopy		2B	3B

Fig. 22.6 Global radiation for the five climatic models. (Source: Own elaboration 2019)

The three models above the tree canopy (1, 2A, and 2B) follow similar curves coherent with the particularities of each methodology. In curve 2A the climatic particularities of the day within some hours were partially cloudy. These particularities also reflect on curve 2B. As for ENVI-met results, on curve 3B as per the simulation motor calculated from 2:00 p.m., the tree canopy no longer shadows the evaluated point, as values rise to couple with 3A curve (above the tree canopy).

22.3 Impact of Local Urban Climate on Building Energy Performance

Five simulation sequences were run in the validated BSM (EnergyPlus) with the established microclimatic models:

– One simulation sequence for model 1 (this model does not distinguish the relative position of the housing unit above or under the tree canopy): Units in the first floor, fifth floor, and eighth-upper floor
– Two simulation sequences for model 2: Housing unit in the first floor with model 2B (below the tree canopy) and units in the fifth and eighth floors with model 2A (above the tree canopy)

– Two simulation sequences for model 3: Housing unit in the first floor with model 3B (below the tree canopy) and units in the fifth and eighth floors with model 3A (above the tree canopy)

Figure 22.7 shows interior temperature and Fig. 22.8 shows energy consumption results for each model. The housing units simulated with climatic model 1 (statistical data) have the following characteristics: average temperature of the case of the first floor under tree canopy is 24.1 °C, and for cases above the tree canopy, the average temperature of the fifth level is 26.8 °C and that of the eighth and upper level is 30.3 °C. The energy consumptions for cooling per square meter were 0.16, 1.75, and 12.06 kWh/m^2, respectively.

Results of simulations with the climatic model 2 (monitored data) are average temperatures of 25.8 °C at the first level under tree canopy, and of 29.9 and 31.1 °C for cases of the fifth level and the eighth and upper level. Consumptions were 0.64, 4.28, and 25.87 kWh/m^2, respectively.

The resulting values simulated with climatic model 3 (ENVI-met) are average temperatures of 26.9 °C in the case of the first floor under tree canopy, 32.2 °C in the fifth level, and 36.9 °C in the eighth and upper level above the tree canopy. The consumptions in these cases were 0.89, 4.38, and 23.96 kWh/m^2, respectively.

Evaluation of the housing unit performance with climatic model 1 results in the lowest indoor temperatures and energy consumption. These are also the farther apart from in situ data obtained through monitoring the existing housing units. The underestimation of energy consumption presents differences of more than 50% of monitored values that double the simulated results. This is explained because of the averaged climatic information that flattens the curve and uncovers the climate change effect. Also the heat island effect is not taken into account as climatic data was taken outside the city. Moreover, without a differentiation of the relative height of the housing unit, particularities of the microclimate of the city of Mendoza are also omitted.

On the other hand, the results given with the ENVI-met model (3A and 3B) are very close to those of the monitored models (2A and 2B) with differences of ±3.5%. This study reveals the capabilities and advantages of working with this tool for the generation of microclimatic data, which when integrated with EnergyPlus presents a less expensive and fast alternative to in situ monitoring.

In conclusion, theoretical models of urban microclimatic simulation are an adequate and necessary tool to be able to not only diagnose the thermo-environmental behavior of an outdoor area, but also predict the building behavior inserted in a given existing urban configuration or proposed scenario.

The results of the study demonstrate the reliability of the proposed method. A combination of ENVI-met and EnergyPlus increases the simulation accuracy in terms of interior temperatures and energy consumption. The coupling of the urban and building dynamic prediction software can be performed all year round following the same methodology.

If local in situ temperatures are not available for the assessment, ENVI-met offers a valid option to climatic 10/20 years' averaged local data. The average climatic data is lower than real on-site measurements on the one hand, because it is

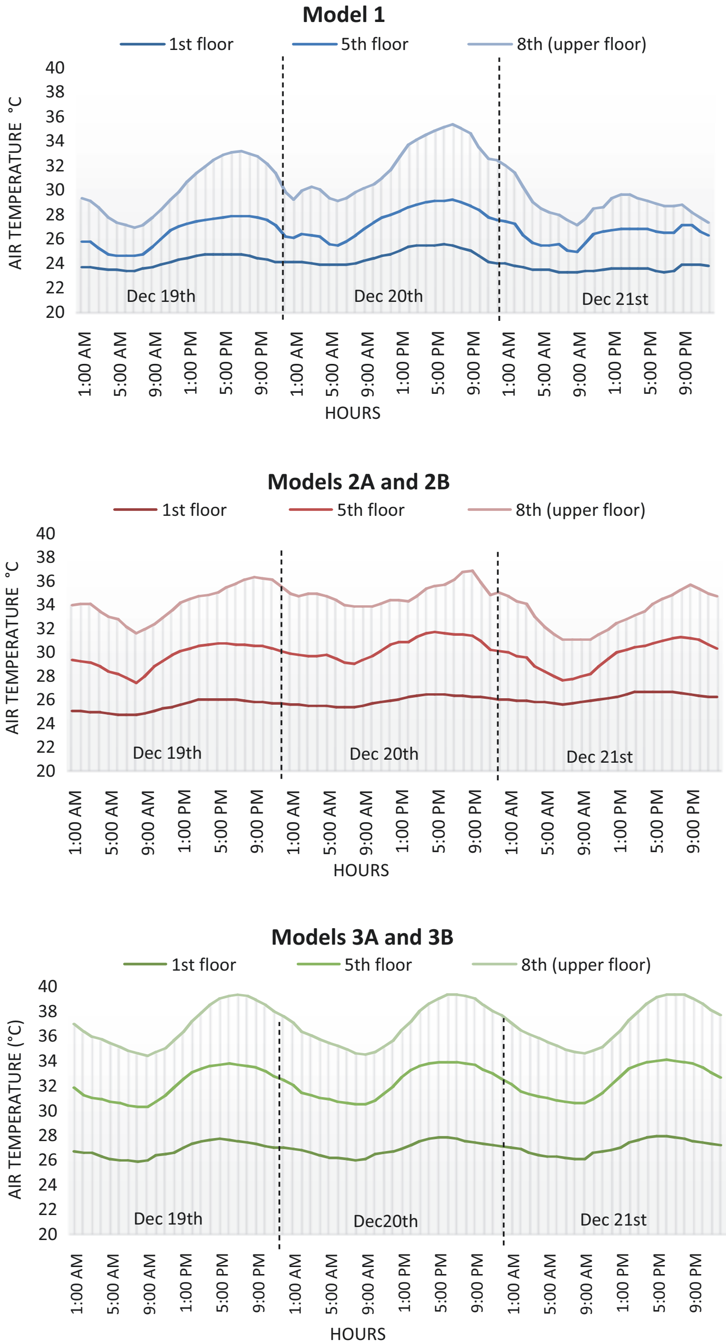

Fig. 22.7 Interior temperatures of the studied housing units. Model 1 for the first, fifth, and eighth floors. Model 2A for the fifth and eighth floors and model 2B for the first floor. Model 3A for the fifth and eighth floors and model 3B for the first floor. (Source: Own elaboration 2019)

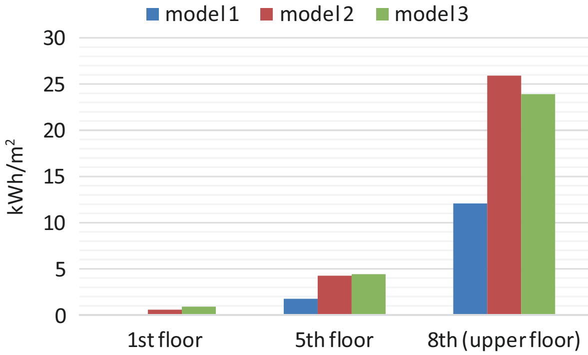

Fig. 22.8 Energy consumption of the studied housing units. Model 1 for the first, fifth, and eighth floors. Model 2A for the fifth and eighth floors and model 2B for the first floor. Model 3A for the fifth and eighth floors and model 3B for the first floor. (Source: Own elaboration 2019)

usually taken outside the city in airports that are not affected by the urban heat island, and on the other hand, because averages tend to uniform temperatures.

Data generated in this study by linking the microclimatic model ENVI-met to the building energy simulation program EnergyPlus demonstrated the importance of more robust and multi-scale approaches for achieving high-accuracy investigations on the impact of local urban climate on building energy performance.

References

Abbasabadi, N., & Ashayeri, M. (2019). Urban energy use modeling methods and tools: A review and an outlook. *Building and Environment, 161*, 106270.

Alchapar, N. L., Correa, E. N., & Cantón, M. A. (2014). Classification of building materials used in the urban envelopes according to their capacity for mitigation of the urban heat island in semiarid zones. *Energy and Buildings, 69*, 22–32.

Balter, J. (2015). *Sustentabilidad de edificios en altura en Ciudades-Oasis. Características arquitectónicas y ambientales para el caso de la ciudad de Mendoza*. PhD thesis. Universidad Nacional de La Plata.

Balter, J., Ganem Karlen, C., & Cantón, M. A. (2013). Evolución morfológica y materialización en edificios en altura en la ciudad de Mendoza. Incidencias en el comportamiento térmico interior. *Revista Área, 19*, 8–25.

Balter, J., Alchapar, N. L., Correa, E. N., & Ganem Karlen, C. (2018). Validation of microclimatic model calculated with ENVI-met as a tool for thermal building analysis of EnergyPlus. In *Proceedings of the 5th International Congress on Building Simulation. IBPSA—International Building Performance Simulation Association*.

Bruse, E. (2006). ENVI-met 3.1. On-Line manual. Retrieved from http://www.envi-met.com

Cantón, M. A., Mesa, A., Cortegoso, J. L., & de Rosa, C. (2003). Assessing the solar resource in forested urban environments. *Architectural Science Review, 24*, 115–123.

Ciancio, V., Falasca, S., Golasi, I., Curci, G., Coppi, M., & Salata, F. (2018). Influence of input climatic data on simulations of annual energy needs of a building: EnergyPlus and WRF modeling for a case study in Rome (Italy). *Energies, 11*(10), 2835.

Coakley, D., Raftery, P., & Keane, M. (2014). A review of methods to match building energy simulation models to measured data. *Renewable and Sustainable Energy Reviews, 37*, 123–141.

Correa, E. N. (2006). *Isla de Calor Urbana. El caso del área metropolitana de Mendoza*. PhD thesis. Facultad de Ciencias Exactas. Área Energías Renovables. Universidad Nacional de Salta.

Davies, M., Steadman, P., & Oreszczyn, T. (2008). Strategies for the modification of the urban climate and the consequent impact on building energy use. *Energy Policy, 36*(12), 4548–4551.

DOE—Department of Energy US. United Nations Population Division. (2017). *World population prospects: The 2017 revision, key findings and advance tables*.

Ganem Karlen, C. (2006). *Rehabilitación ambiental de la envolvente de viviendas. El caso de Mendoza*. PhD thesis. Escuela Técnica Superior de Arquitectura de Barcelona. Universidad Politécnica de Cataluña. Barcelona Tech.

Grossi Gallegos, H., Nollman, U., Lopardo, R., & Atienza, G. (1983). Evaluación preliminar del recurso solar en Argentina. *Actas de 8° ASADES, 1*, 179–194.

Hong, T., Chen, Y., Luo, X., Lou, N., & Lee, S. H. (2020). Ten questions on urban building energy modelling. *Building and Environment, 168*, 106508.

IEA—International Energy Agency. (2014). World energy outlook 2014.

IPCC—International Panel on Climate Change. (2014). *Climate change 2014: Synthesis report. Contribution of working groups I, II and III to the fifth assessment report of the Intergovernmental Panel on Climate Change*. Geneva: IPCC.

Kolher, N., & Hassler, U. (2002). The building stock as a research object. *Building Research & Information, 30*, 226–236.

Kottek, M., Grieser, J., Beck, C., Rudolf, B., & Rubel, F. (2006). World map of the Köppen-Geiger climate classification update. Sustainable United Nations. *Meteorologische Zeitschrift, 15*, 259–253.

Kuo-Tsang, H., & Yi-Jhen, L. (2017). Impact of street canyon typology on building's peak cooling energy demand. *Energy and Buildings, 154*, 448–464.

Lassandro, P., & di Turi, S. (2019). Multi-criteria and multiscale assessment of building envelope responsibility to rising heat waves. *Sustainable Cities and Society, 51*, 101755.

Lauzet, N., Rodler, A., Musy, M., Azamde, M. H., Guernouti, S., Mauree, D., & Colinart, T. (2019). How building energy models take the local climate into account in an urban context—A review. *Renewable and Sustainable Energy Reviews, 116*, 109390.

Levermore, G., Parkinson, J., Lee, K., Laycock, P., & Lindley, S. (2017). The increasing trend of the urban heat island intensity. *Urban Climate, 24*, 360–368. https://doi.org/10.1016/j.uclim.2017.02.004.

Longobardi, M., & Hancock, M. (2000). Field trip strategies. In *Proceedings of TIA, Oxford*.

Manley, G. (1958). On the frequency of snowfall in metropolitan England. *Quarterly Journal of the Royal Meteorological Society, 84*(359), 70–72.

Martinez, C., Ruiz, M., & Atencio, L. (2017). Proyecto integral de forestación y reforestación urbana para Mendoza. Sustenta-bilidad ambiental del bosque urbano para ciudades de zonas áridas de Argentina—Etapa 1 UNICIPIO—Provincia de Mendoza. *Instituto de Ambiente, Hábitat y Energía INAHE – CCT CONICET Mendoza, 1*, 96.

Mauree, D., Naboni, E., Coccolo, S., Perera, A. T. D., Nik, V. M., & Scartezzini, J. L. (2019). A review of assessment methods for the urban environment and its energy sustainability to guarantee climate adaptation of future cities. *Renewable and Sustainable Energy Reviews, 112*, 733–746.

Moonen, P., Defraeye, T., Dorer, V., Blocken, B., & Carmeliet, J. (2012). Urban physics: Effect of the micro-climate on comfort, health and energy demand. *Frontiers of Architectural Research, 1*(3), 197–228.

Morakinyo, T. E., Dahanayake, K. W. D., Adegun, O. B., & Balogun, A. A. (2016). Modelling the effect of tree shading on summer indoor and outdoor thermal condition of two similar buildings in a Nigerian university. *Energy and Buildings, 130*, 721–732.

OB Org—One Building Organization. (2019). *Repository of free climate data for building performance simulation*. Retrieved from http://climate.onebuilding.org/

Oke, T. R. (2004). *Initial guidance to obtain representative meteorological observations at urban sites. Iom Report*. Geneva: World Meteorological Organization.

Pastore, L., Corrao, R., & Heiselberg, P. K. (2017). The effects of vegetation on indoor thermal comfort: The application of a multi-scale simulation methodology on a residential neighborhood renovation case study. *Energy and Buildings, 146*, 1–11.

Perini, K., Ottelé, M., Giulini, S., Magliocco, A., & Roccotiello, E. (2017). Quantification of fine dust deposition on different plant species in a vertical greening system. *Ecological Engineering, 100*, 268–276.

Ruiz, M. A., Sosa, M. B., Correa, E. N., & Cantón, M. A. (2017). Design tool to improve daytime thermal comfort and nighttime cooling of urban canyon. *Landscape and Urban Planning, 167*, 249–256.

Schwed, D., & Sheng, M. (2017). Assessment of the annual energy demand for cooling of buildings in their urban context in 26 cities in China. *Procedia Engineering, 198*, 305–312.

SMN. Servicio Meteorológico Nacional Argentino [National Weather Service of Argentina] (2019). Fuerza Aérea Argentina. Ministerio de Defensa.

UN. United Nations (2017). *United Nations framework convention on climate change, initiatives in the area of human settlements and adaptation*. Retrieved from https://unfccc.int/news/rapidurbanization-increases-climate-risk-for-billions-of-people

van Hooff, T., Blocken, B., Timmermans, H. J. P., & Hensen, J. L. M. (2016). Analysis of the predicted effect of passive climate adaptation measures on energy demand for cooling and heating in a residential building. *Energy, 94*, 811–820.

Xu, T., Sathaye, J., Akbari, H., Garg, V., & Tetali, V. (2012). Quantifying the direct benefits of cool roofs in an urban setting: Reduced cooling energy use and lowered greenhouse gas emissions. *Building and Environment, 48*, 1–6.

Yang, X., Zhao, L., Bruse, M., & Meng, Q. (2012). An integrated simulation method for building energy performance assessment in urban environments. *Energy and Buildings, 54*, 243–251.

Zinzi, M., Carnielo, E., & Mattonia, B. (2018). On the relation between urban climate and energy performance of buildings. A three-years experience in Rome, Italy. *Applied Energy, 221*, 148–160.